American Mineralogist, Volume 64, pages 274–287, 1979

Trace-element partitioning between garnet peridotite minerals and water-rich vapor: experimental data from 5 to 30 kbar

BJØRN O. MYSEN

Geophysical Laboratory, Carnegie Institution of Washington
Washington, D. C. 20008

Abstract

The values of individual rare earth element (REE) partition coefficients (weight ratio, $C_{REE}^{vapor}/C_{REE}^{crystal} = K_{REE}^{vapor-crystal}$) range between 1 and 200 for garnet, clinopyroxene, orthopyroxene, and olivine in equilibrium with H_2O-rich vapor under experimental conditions corresponding to those of the upper mantle. The $K_{REE}^{vapor-crystal}$ increases rapidly with increasing PH_2O (*e.g.*, $K_{Sm}^{vapor-Cpx}$ = 0.01, 3, 12 and 31, respectively, at 5, 10, 20, and 30 kbar). Calculated bulk partition coefficients (as defined by Shaw, 1970) range from 5 to 250 for an average garnet peridotite assemblage in the pressure range 5–40 kbar, with $D_{Ce}^{vapor-rock} > D_{Tm}^{vapor-rock}$

The portions of the upper mantle sampled and brought to the surface by kimberlite magma characteristically display garnet contents ranging from near zero to about 20 percent. If a suite of such garnet peridotites equilibrated with H_2O-rich vapor, a wide range of absolute REE contents and degree of light REE enrichment would result. It is notable that the more depleted garnet peridotite nodules in kimberlite (also the most garnet-poor) commonly show great light-REE enrichment (Ce/Yb $\geq$ 10), as would be expected if these rocks have suffered metasomatic alteration.

Andesites in island arcs commonly show considerable light-REE enrichment (Ce/Yb =2.5–10). It is argued here that the peridotite wedge overlying a descending plate of oceanic basaltic composition with an eclogitic mineral assemblage would attain considerable light-REE enrichment as a result of equilibration with H_2O-rich vapor released by dehydration of the material in the descending slab. If, for example, 0.5 weight percent H_2O was released and initially equilibrated with an eclogitic rock before migrating into the overlying peridotite, the peridotite (with an initially unfractionated REE pattern) could attain Ce/Sm and Ce/Tm ratios near 3 and 5 respectively. Partial melting of this hydrated peridotite would result in melts of andesitic bulk composition with Ce/Sm = 3–4 and Ce/Tm ~ 10, closely resembling the REE patterns found in andesites in island arcs.

Introduction

The presence of volatile components in the upper mantle (H_2O, CO_2, S, *etc.*) has been documented by, for example, Oxburgh (1964), Anderson (1975), and Muenow *et al.* (1977). (For review of other data see also Irving and Wyllie, 1975, and Boettcher *et al.*, 1975.) As a result of these observations, extensive experimental work has been carried out on the effects of volatiles on phase relations of upper mantle materials (*e.g.*, Yoder, 1969; Kushiro, 1969, 1972; Kushiro *et al.*, 1968; Eggler, 1973, 1974, 1975, 1976; Huang and Wyllie, 1976; Mysen and Boettcher, 1975a, b). With a few notable exceptions (*e.g.*, Rubey, 1955), relatively little attention has been drawn to the source of volatiles in the upper mantle, to their migration rates, and to the transport capacity of such volatiles for silicate components.

Evidence from volcanic rocks suggests heterogeneous distribution of volatiles in the source regions of partial melts in the upper mantle. Mid-oceanic ridge basalts appear to be essentially H_2O-free, for example (Delaney *et al.*, 1977), whereas volcanic rocks in island arcs contain several percent H_2O (*e.g.*, Anderson, 1975; Muenow *et al.*, 1977). Kimberlite contains large amounts of both CO_2 and H_2O.

A consequence of heterogeneous distribution of

0003–004X/79/0304–0274$02.00

volatiles in the source region of melts in the upper mantle is the possibility of migration of these volatiles. Unfortunately, experimental data bearing on infiltration of fluids in crystalline upper mantle are scarce. Marsh (1976a) suggested that H_2O may be essentially immobile, whereas preliminary experimental data of Mysen *et al.* (1977) indicate that an H_2O-rich front may infiltrate crystalline mantle materials at the rate of several millimeters per hour at pressures above 15 kbar. Thus, an H_2O-rich phase (as contrasted with H_2O bound in crystalline materials or silicate liquid) may act as a transporting agent of silicate components in the upper mantle, provided significant amounts of silicate components can dissolve in such fluids.

Some evidence suggests large solubilities (several tens of a weight percent) of major elements in H_2O-rich fluids under pressure conditions corresponding to those of the upper mantle (Burnham, 1967; Nakamura and Kushiro, 1974; Eggler and Rosenhauer, 1978). Cullers *et al.* (1973) and Zielinski and Frey (1974) measured partitioning of REE between H_2O-rich vapors and some peridotite minerals at 1–2 kbar, and concluded that the REE were strongly partitioned into the crystals under the low-pressure conditions of their experiments. Some major-element data of Kennedy *et al.* (1962), Burnham (1967), and Eggler and Rosenhauer (1978) indicate that the solubility of silicate components in H_2O-rich fluids depends strongly on pressure. The low-pressure data of Cullers *et al.* (1973) and Zielinski and Frey (1974), therefore, may not be applicable to upper mantle pressures.

In view of the importance attributed to knowledge of the trace-element contents of potential parental rocks of partial melts in the upper mantle, an understanding of the processes governing their distribution patterns is needed. Consequently, partition coefficients involving a water-rich vapor and the constituent minerals of garnet peridotite have been determined for representative REE as a function of pressure. These data were then used to evaluate the role of metasomatic alteration of the distribution patterns of these elements in the upper mantle.

Experimental technique

Starting materials were synthetic pyrope (Ga) and diopside (Cpx) either with or without the trace element in solution. The starting material was ground to less than 5 μm grain size and run in sealed Pt capsules together with H_2O containing a radioactive trace element. Reversal experiments were carried out by taking a split of an experimental run product, washing it in alcohol, drying it, and running it together with tracer-free, double-distilled H_2O in a sealed Pt capsule. The minerals grew to about 10 μm grain size during a forward experiment, so the starting material was reground to less than 5 μm before the reversal experiment was carried out. Reversal experiments are marked with asterisks in the run table (Table 1).

All experiments were conducted at 1100°C in the pressure range 5–30 kbar. An internally-heated gas-media apparatus (Yoder, 1950) was used at $P \leq 10$ kbar, whereas a solid-media high-pressure apparatus (Boyd and England, 1960) was used at higher pressures. Pressures in the solid-media high-pressure apparatus were corrected by −4 percent as calibrated against the quartz–coesite transition.

Vapor–crystal partition coefficients were determined by analyzing the crystals and determining the trace-element content of the coexisting vapor by mass balance. Cerium, samarium, and thulium, respectively, were chosen as representative light, intermediate, and heavy REE. Analyses were conducted

Table 1. Experimental results at 1100°C

Run no.	Pressure, kbar	Run duration, hours	Wt % H_2O	Crystal and element	Concentration, ppm		$K^{H_2O\text{-crystal}}$
					Vapor	Crystal	
615	20	95	12.60	Di(Sm)	160±15	14±1	11±1.3
616*	20	96	23.19	Di(Sm)	37±4	2.8±0.2	13±2
620	20	92.5	12.84	Di(Tm)	18±2	1.0±0.1	18±2.5
623*	20	96	15.00	Di(Tm)	4.4±0.4	0.23±0.02	19±2.4
661	30	96	6.66	Di(Sm)	254±18	8.3±0.5	31±3
662	5	98	4.08	Di(Sm)	0.25±0.25	17.4±0.9	0.01±0.01
664	10	121	4.36	Di(Sm)	50±3	14.6±0.5	3.4±0.2
673	20	96.5	9.46	Py(Sm)	64±6	32±3	2.0±0.3
679	20	93	9.61	Py(Tm)	0.104±0.007	0.189±0.011	0.55±0.05
690	20	89	18.83	Py(Ce)	8180±200	71±6	115±10

**Reversal experiment (trace element in crystal prior to experiment).*

with the beta-track mapping technique (Mysen and Seitz, 1975), using cerium-141, samarium-151, and thulium-171 as sources of beta particles. Standards for the trace element analyses were $NaAlSi_3O_8$ glasses with known amounts of trace element added.

The theoretical uncertainty (exposure time and statistical uncertainties) of an analysis of a mineral (1σ) is approximately 4 percent (relative). Most analyses of minerals from experimental runs have uncertainties within this limit. It is concluded, therefore, that homogeneous grains were obtained with the run duration of 4 days used in these experiments. The weighing error in calculating the trace-element content of the vapor by mass balance (including loss of fluid during welding) is less than 5 percent (relative). Consequently, the analytical uncertainty of a vapor–crystal partition coefficient determined by this method is of the order of 6 percent (1σ).

The results (calculated as partition coefficients) of the reversal experiments with diopside were generally within 10 percent of the original value. A minimum value for the diffusion coefficient of Sm in diopside at 1100°C can be estimated from the run length and grain size of the crystals ($\sim 10\ \mu m$). The coefficient is equal to or greater than 10^{-15} cm²/sec. This value compares with about 10^{-14} cm²/sec calculated by Zielinski and Frey (1974) for Gd^{3+} in diopside at 800°C. Diffusion coefficients of the individual REE in garnet peridotite minerals are unlikely to vary by more than an order of magnitude. It is concluded, therefore, that because 4 days run duration was sufficient to attain equilibrium with Sm in diopside, the same run duration is also sufficient to attain equilibrium with the other REE in diopside and other garnet peridotite minerals. This conclusion is further substantiated by the observation that *all* minerals were compositionally homogeneous after an experiment.

Partition coefficients for olivine–vapor and orthopyroxene–vapor were calculated from REE clinopyroxene–olivine and clinopyroxene–orthopyroxene partition coefficients derived from the data of Mysen (1977a), which were obtained at 20 kbar in the temperature range 960°–1075°C. Details of this calculation are described below. The temperature-dependence of these partition coefficients is small in the temperature range considered, and no temperature correction was applied to the values when the data of Mysen (1977a) were extrapolated to 1100°C. The relative uncertainty of the partition coefficients of Mysen (1977a) is about 5 percent (1σ), resulting in an estimated relative uncertainty of the calculated vapor–crystal partition coefficients, $K_{REE}^{H_2O-Ol}$ and $K_{REE}^{H_2O-Opx}$, of about 8 percent.

Another important aspect of the experiments reported here is the solubility behavior of the mineral in H_2O-rich vapor. The experimental part of this study involved pyrope ($Mg_3Al_2Si_3O_{12}$) and diopside ($CaMgSi_2O_6$). Eggler and Rosenhauer (1978) reported that even though 10–15 weight percent $CaMgSi_2O_6$ was dissolved in H_2O in the pressure range 20–30 kbar, no evidence was found for incongruent solution of diopside in the vapor in this pressure range. Electron microprobe analysis of diopside after an experiment in my study did not reveal nonstoichiometry, thus supporting the conclusion of Eggler and Rosenhauer (1978). Less information is available on the solubility behavior of pyrope in H_2O-rich vapor at high pressure. The starting material (kindly supplied by R. C. Newton, University of Chicago) was crystallized under hydrothermal conditions at 1000°C and 28 kbar. Electron microprobe analysis of this starting material as well as analysis of the pyrope after an experiment did not show nonstoichiometry within the uncertainty of the analysis (2–3 percent, relative). Furthermore, optical examination of the run products indicated that pyrope was the only stable crystalline phase present. I conclude, therefore, that both diopside and pyrope dissolve congruently in coexisting H_2O-rich fluid under the pressure and temperature conditions of the present experiments.

Results

Experimental results are listed in Table 1, in which reversal experiments are marked with asterisks. A comparison of values for $K_{REE}^{H_2O-crystal}$ ($=C_{REE}^{H_2O}/C_{REE}^{crystal}$) for various garnet peridotite minerals at 20 kbar and 1100°C is shown in Figure 1. Two features of the data warrant comment. First, with the exception of $K_{Tm}^{H_2O-Ga}$, the REE are partitioned into the H_2O-rich vapor relative to the crystalline phases. Second, the partition coefficients vary with the atomic number of the REE.

The pressure-dependence of the vapor–crystal partition coefficients has been evaluated for diopside using Sm at 1100°C (Fig. 2). The uncertainty of the results derived with the mass-balancing method used to determine the trace-element contents of the vapors increases as the trace-element concentration in the vapor decreases. For the experimental technique used here, the sensitivity corresponds to $K_{REE}^{H_2O-crystal} \sim 0.01$ in the pressure range of the internally-heated gas-media apparatus. Because of the smaller volume used in the solid-media high-pressure apparatus, experiments with that apparatus result in even lower sensitivity (cor-

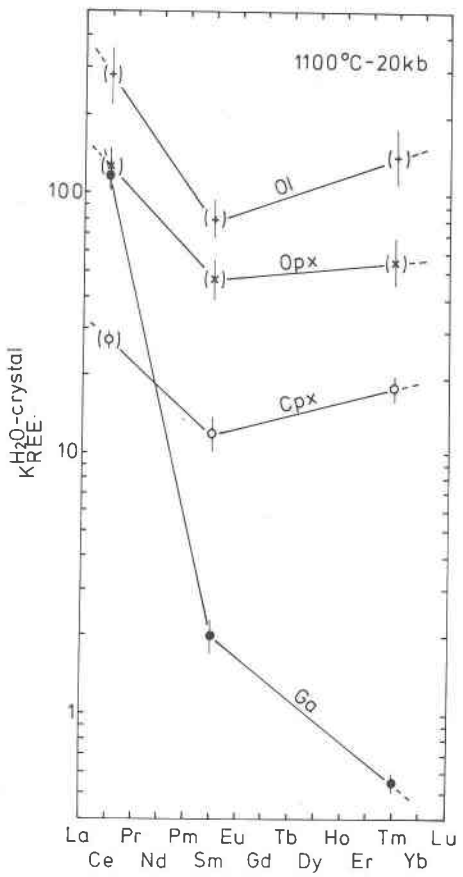

Fig. 1. Vapor–crystal partition coefficients for garnet, clinopyroxene, orthopyroxene, and olivine at 20 kbar and 1100°C. Symbols in parentheses represent calculated partition coefficients. Error bars, $\pm 1\sigma$.

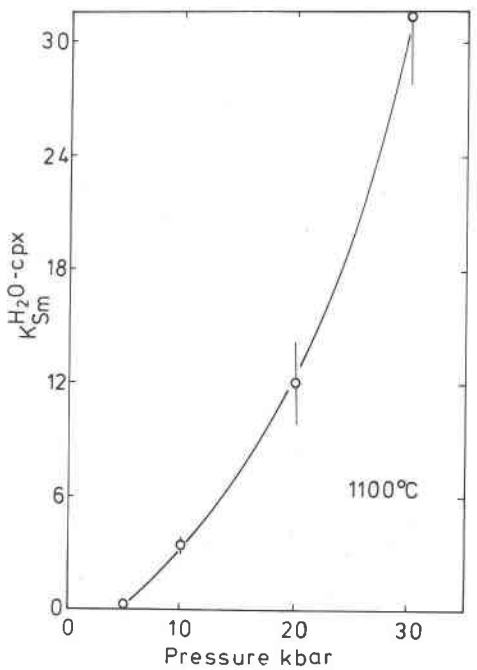

Fig. 2. Vapor–diopside partition coefficients for samarium as a function of pressure at 1100°C. Error bars, $\pm 1\sigma$.

responding to $K_{REE}^{H_2O-crystal} \sim 0.1$). The data in Table 1 show that no Sm was detected in the vapor at 5 kbar. Maximum values for other REE partition coefficients at 5 kbar are listed together with $K_{Sm}^{H_2O-diopside}$ in Table 2. A very strong pressure-dependence of the Sm vapor–crystal partition coefficients is evident from the data in Figure 2. The low-pressure data are comparable to those of Cullers *et al.* (1973) and Zielinski and Frey (1974) at pressures below 5 kbar. There are no other published experimental data with which to compare the present results at pressures corresponding to those of the lower crust and upper mantle.

The data shown in Figures 1 and 2 may be used to calculate vapor–crystal partition coefficients for other REE and other garnet peridotite minerals, provided the individual REE are not fractionated by the vapor and REE crystal–crystal partition coefficients are available for the minerals and REE in question. Information on the temperature- and pressure-dependence of crystal–crystal partitioning is also necessary for extrapolation of $K_{REE}^{H_2O-crystal}$ to suitable pressure and temperature conditions. The only data on the pressure-dependence of REE crystal–crystal partitioning in the pressure range considered here (corresponding to the upper mantle) are those of Mysen (1977a) for coexisting olivine and aluminous enstatite at 10 and 20 kbar. No dependence was seen. The following calculations assume that other crystal–crystal partition coefficients (K_{REE}^{Cpx-Ga}, $K_{REE}^{Cpx-Opx}$, and K_{REE}^{Ol-Cpx}) do not vary in the pressure range 5–30 kbar. This assumption may not be completely justified, in view of the large volume changes that probably accompany solution of REE in garnet peridotite minerals relative to the REE-free analogs. It is probable, however, that whatever the relative pressure-dependence of $K_{REE}^{crystal-crystal}$ may be, it is the same for all REE because of their similar size and valence. Consequently, if an error

Table 2. Maximum values of Ce, Sm, and Tm partition coefficients at 1100°C and 5 kbar

	Ce	Sm	Tm
Olivine	0.2	0.1	0.08
Orthopyroxene	0.05	0.04	0.06
Clinopyroxene	0.02	0.01	0.02

is introduced because of this assumption, it affects only the absolute abundances and not frationation of REE. It is likely, therefore, that the conclusions reached here (see below) will not be significantly altered after the pressure-dependence of $K_{REE}^{crystal-crystal}$ becomes known.

If there is no fractionation of the individual REE in an H_2O-rich vapor, data on one $K_{REE}^{H_2O-crystal}$ and the REE crystal–crystal partition coefficients for the other minerals can be used to calculate other $K_{REE}^{H_2O-crystal}$. Consequently, if two sets of vapor–crystal partition coefficients are known and one of these sets can also be reproduced by calculation based on the other set, it can be concluded that the vapor does not fractionate between the individual REE. The results of such an exercise are shown in Table 3, using $K_{Sm}^{H_2O-Ga}$ and the data of Mysen (1977a) for K_{REE}^{Cpx-Ga}. The comparison of these results suggests that the individual REE are not fractionated by H_2O-rich vapor.

From the above considerations, it is tentatively concluded that the strong positive pressure-dependence measured for $K_{Sm}^{H_2O-diopside}$ is caused by the increasing solubility of REE in H_2O-rich vapor, and that the same pressure-dependence is to be expected for other REE when other minerals are considered. It may be argued that the REE in the vapor may form complexes with cations from the major-element silicates. No data are available in support of this suggestion. This possibility, therefore, is not taken into account in the following discussion. It is then possible to calculate all REE vapor–crystal partition coefficients as a function of pressure, provided that the different solubilities of major element components in the vapor are neglected. The neglect of major elements dissolved in the vapor is justified in view of the fact that the mole fraction of H_2O in the fluids is of the order of 0.94–0.98, depending on whether the dissolved silicate components are calculated as oxides or $CaMgSi_2O_6$, respectively. It is assumed that this small silicate impurity in the vapor does not significantly affect the REE solubility in the fluid. The

Table 3. Comparison of measured and calculated $K_{REE}^{H_2O-diopside}$ at 1100°C and 20 kbar

	Sm	Tm
Measured	12±1.5	18.5±2.5
Calculated	13±3	21±3

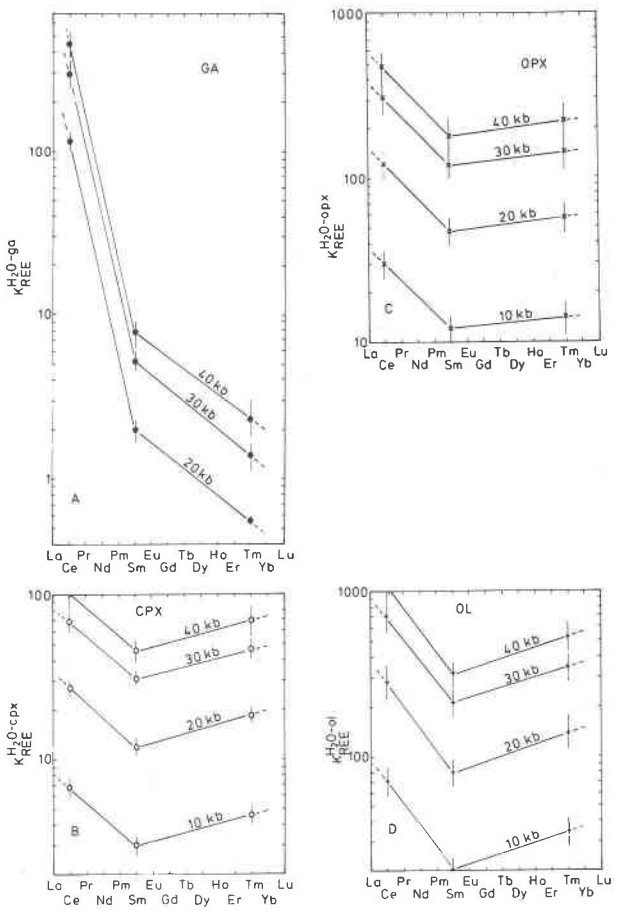

Fig. 3. Pressure dependence of $K_{REE}^{H_2O-crystal}$ at 1000°C for olivine, orthopyroxene, clinopyroxene, and garnet. Error bars, $\pm 1\sigma$.

results of such calculations are shown in Figure 3. The 40-kbar curves are based on an extrapolation of $K_{Sm}^{H_2O-diopside}$ to 40 kbar (see Fig. 2). The results of these calculations show that a water-rich fluid in the upper mantle constitutes a major sink for REE. This observation is further substantiated by the calculated bulk partition coefficients for two model garnet peridotites (Table 4) shown in Figure 4. The results in this figure show that the water-rich fluid is strongly enriched in light REE, and that the degree of light-REE enrichment increases with increasing modal garnet content of the rock. The absolute REE abundance of the fluid will also increase rapidly with pressure if the assumptions based on the vapor–diopside partitioning data are appropriate. The bulk partition coefficient involving garnet-free peridotite and water-rich vapor does not vary significantly with atomic number because none

Table 4. Compositions of garnet peridotites (weight percent)

	GP1	GP1(5)	GP1(10)	GP1(16)	GP2
SiO_2	47.6	47.4	47.3	47.0	47.8
Al_2O_3	2.5	1.9	1.1	<0.1	5.1
MgO	47.3	48.5	49.9	52.0	44.5
CaO	2.6	2.2	1.7	1.0	2.6
		Modal Compositions			
Ga	10	7.3	4.2	0.1	20
Cpx	10	8.3	6.5	4.0	10
Opx	20	20.6	21.3	22.1	20
Ol	60	63.8	68.0	73.8	50
		REE Contents*			
Ce	1	0.45	0.17	0.04	1
Sm	1	0.91	0.77	0.45	1
Tm	1	0.99	0.96	0.72	1

Relative to average chondrite (Schmitt et al., 1963, 1964).

of the minerals in such a peridotite fractionate significantly between the individual REE.

Petrological implications

Stable continental shields

Direct evidence for heterogeneous distribution of trace elements in the upper mantle is found in garnet peridotite nodules from kimberlite and related rocks in southern and central Africa (Shimizu, 1975a, b; Ridley and Dawson, 1975; Mitchell and Carswell, 1976). Evidence for isotopic heterogeneities is given by Ridley and Dawson (1975) and Erlank and Shimizu (1977). Petrographic descriptions of secondarily-grown[1] phlogopite and potassic richterite are given by, for example, Dawson and Powell (1969), Erlank (1973), Aoki (1974), and Erlank and Rickard (1977).

Data supporting an interpretation of metasomatic alteration of peridotite trace element contents and isotope geochemistry *in* the mantle *prior to* transport of the samples of such mantle to the earth's surface are provided by Ridley and Dawson (1975), Rhodes and Dawson (1975), and Erlank and Shimizu (1977). The REE data of Shimizu (1975a) are also best interpreted in terms of metasomatism in the mantle prior to sampling by ascending kimberlite magma.

As mentioned previously, two types of garnet peridotite occur in the portions of the upper mantle sampled by kimberlite beneath the South African craton. The granular nodules show evidence of major-element depletion perhaps resulting from partial melting. The sheared nodules are not depleted in major elements (these two types of peridotite nodules are referred to as depleted and fertile, respectively). This distinction is not seen in the REE patterns (Shimizu, 1975a,b; Ridley and Dawson, 1975; Mitchell and Carswell, 1976). The contrast between major and trace elements is perhaps best illustrated by the REE patterns of a sheared and a granular garnet peridotite nodule (Fig. 5). These data show a considerable relative light-REE enrichment of the depleted granular nodule (352), whereas the sheared fertile nodule (1611) shows an essentially unfractionated REE pattern. The light-REE enrichment is also seen in other depleted garnet peridotite nodules from kimberlite and related rocks (Fig. 5). The patterns of nodules 352, BD 738, and BD 776 are not the result of interaction between the nodules and the host magma during ascent, according to evidence and discussion by the original authors (Shimizu, 1975a; Ridley and Dawson, 1975).

The model used to explain the contrasted major- and trace-element contents of depleted and fertile garnet peridotite is as follows. Consider an upper mantle consisting of fertile peridotite. As the result of partial melting and extraction of the melt from the source region, the residual peridotite after the melting event will acquire a depleted major- and trace-element character. Metasomatic alteration of the depleted material is accomplished by dehydration of minor minerals in neighboring fertile peridotite. The

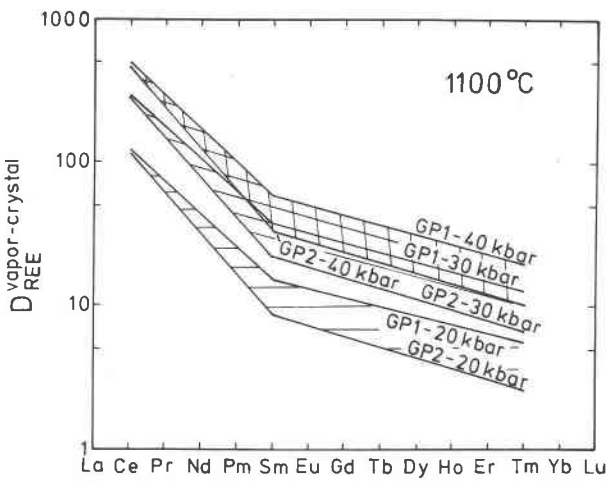

Fig. 4. Bulk partition coefficients, $D^{H_2O-crystal}_{REE}$, for garnet peridotites GP1 and GP2 as a function of pressure as 1100°C. Error bars $\pm 1\sigma$.

[1] Secondary growth is taken to mean formation of a mineral subsequent to equilibration of four-phase peridotite in the upper mantle. The growth could have occurred in the mantle prior to ascent in a magma or as a result of interaction between the nodule and the transporting magma.

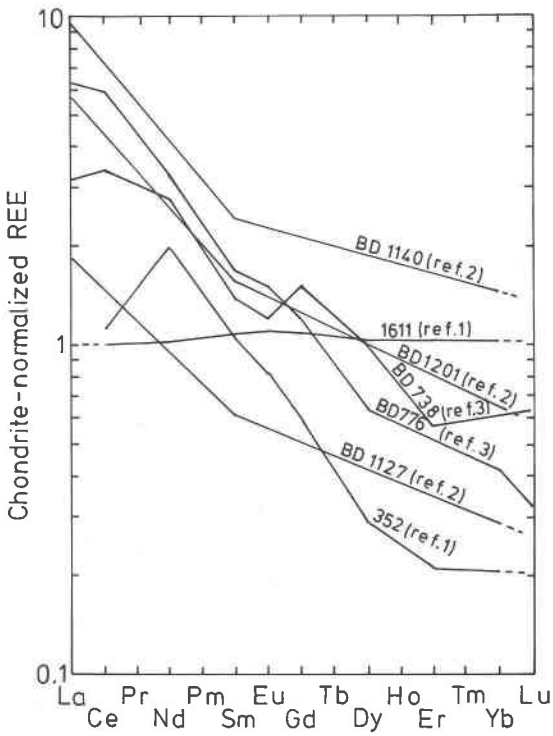

Fig. 5. Published REE patterns of garnet peridotite nodules in kimberlite and related rocks. Ref. 1, Mitchell and Carswell (1976); ref. 2, Shimizu (1975a); ref. 3, Ridley and Dawson (1975).

released fluid will equilibrate with the fertile garnet peridotite and migrate into the neighboring depleted peridotite with which the fluid also equilibrates. The major- and trace-element patterns of depleted garnet peridotite presumably reflect these two processes.

The most important aspects of this model may be assessed by combining the present REE partitioning data with information on melting behavior of garnet peridotite (Kushiro and Yoder, 1974; Mysen and Kushiro, 1977) and mobility of H_2O in the upper mantle (Mysen *et al.*, 1977).

The garnet peridotite nodule 1611 (Nixon and Boyd, 1973) is a likely candidate for the fertile mantle material (*e.g.*, Shimizu, 1975a). According to Mysen and Kushiro (1977), partial melting of garnet peridotite of a composition such as that of 1611 is closely mimicked by the melting behavior observed in simple systems like $CaSiO_3$–$MgSiO_3$–Al_2O_3–SiO_2 (CMAS). By employing the phase-equilibrium data from CMAS (Kushiro and Yoder, 1974), Mysen (1977b) showed that the stoichiometry of the equation expressing the melting of garnet peridotite is approximated by the formulation

$$0.63\ \text{Ga} + 0.41\ \text{Cpx} + 0.09\ \text{Opx} = 0.13\ \text{Ol} + \text{Liq} \qquad (1)$$

The modal composition of the idealized model garnet peridotite, GP1 (Table 4), is similar to that of nodule 1611 (Nixon and Boyd, 1973). In the following calculations, composition GP1 represents the fertile garnet peridotite, and compositions representing various degrees of depletion are derived by melting GP1 with a stoichiometry according to expression (1). With the stoichiometry of equation (1), 16.1 percent melt can be generated from GP1 under invariant conditions. This amount of melting represents the maximum degree of depletion of garnet peridotite GP1.

The equations that describe element concentrations in a metasomatized rock are derived in the Appendix. For a source rock with element concentrations R_i^s and a metasomatized rock with element concentration R_i^D before metasomatism, the concentrations of i in the bulk rock (R_i^M) and the crystalline residue [$(C_i^{xt})^M$] are:

$$R_i^M = R_i^D(1 - Y_v X_M) + \frac{R_i^s X_M Y_v}{D_i^s - X_s(D_i^s - 1)} \qquad (2)$$

and

$$(C_i^{xt})^M = \frac{R_i^M}{(1 - Y_v X_M) + \dfrac{Y_v X_M}{D_i^M}} \qquad (3)$$

In these equations, X_s and X_M are the mass proportions of fluid in source rock and metasomatized rock, respectively. The bulk partition coefficients for source and metasomatized rocks are D_i^s and D_i^M. Finally, the parameter Y_v is the ratio of fluid remaining in the metasomatized rock to equilibrate with it divided by the mass proportion of fluid entering the rock to initiate the metasomatic alteration.

Equations (2) and (3) show that the element concentration of a metasomatized portion of the upper mantle is a complex function of a variety of poorly-known parameters. The results of varying these parameters are shown in Figure 6. In this figure, GP1 is considered the source of metasomatizing fluid. The pressure in all calculations is 40 kbar. The influence of pressure on the element concentrations of the metasomatized rock would be the result of pressure-dependence of the crystal–crystal partition coefficients, and the result of changes in modal proportions of minerals in the rocks because of the pressure-dependence of solid solutions in the minerals (*e.g.*, MacGregor, 1974). It was argued above that the pressure-dependence of crystal–crystal partition coefficients may not be large. No such dependence was therefore considered in the calculations. According to MacGregor, the proportion of garnet would increase

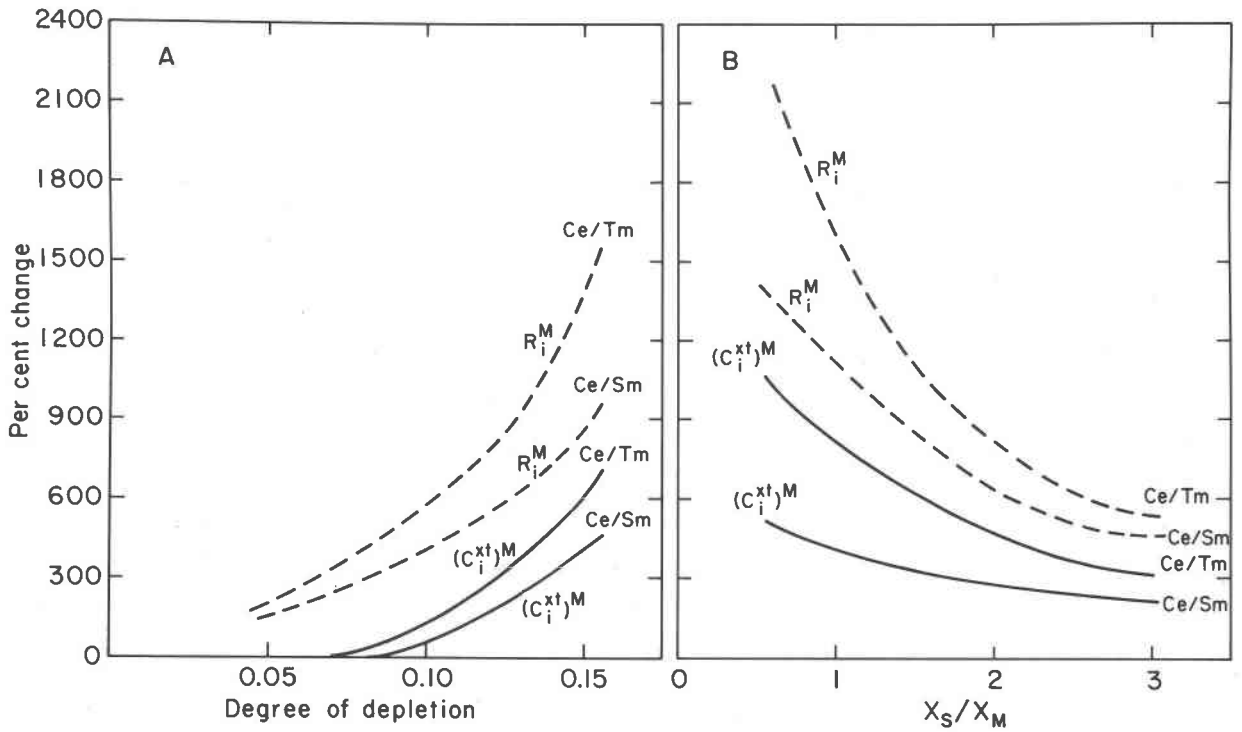

Fig. 6. Degree of change of light REE of metasomatized garnet peridotite [bulk REE (crystals + vapor) − R_i^M·REE content of crystals − $(C_i^{xt})^M$] relative to Ce/Sm and Ce/Tm of unaltered, depleted garnet peridotite. (6A) As a function of degree of depletion [expressed as proportion of fractional melt extracted (F) prior to metasomatism] with $X_s/X_M = 1$, $R_i^s = 1$. (6B) As a function of X_s/X_M with $F = 0.16$ and $R_i^s = 1$.

at the expense of aluminous orthopyroxene with increasing pressure. In GP1 the relative increase of garnet in the range 20–40 kbar would be about 10 percent. This variation will not significantly affect the value of the bulk partition coefficients. It is concluded, therefore, that the results of the calculations approximate the results of metasomatic alteration of garnet peridotite in the upper mantle in the pressure range of garnet peridotite nodules sampled by kimberlite.

All the curves in Figure 6 represent percent change of enrichment factors, Ce/Sm and Ce/Tm, relative to their values after extraction of 5, 10 and 16 percent fractional melt as calculated according to the stoichiometry of equation (1) using the equations of Shaw (1970). The original values of these enrichment factors are given in Table 4.

The effect of modal composition of rock M (depleted GP1) at $X_s/X_M = 1$ and $Y_v = 1$ is shown in Figure 6A. The results show that, as the peridotite rock to be metasomatized becomes more depleted, the degree of light-REE enrichment increases rapidly. The main change of GP1 during depletion is a lowering of garnet content and, to a lesser degree, clinopyroxene content of the rock. Garnet is the only mineral in garnet peridotite that shows significant fractionation of individual REE. Its presence in the metasomatized rock will tend to oppose light-REE enrichment in the rock. The less garnet there is in depleted GP1, the less important this effect will be. Because the garnet content of the residual garnet peridotite decreases as the degree of melting increases, the effect of metasomatism on the REE pattern of the metasomatized rock increases. The effect of the ratio of mass of fluid in source rock and metasomatized rock at $F = 0.16$ and 40 kbar is shown in Figure 6B. The more fluid relative to rock that enters the depleted peridotite, the greater the degree of enrichment. Put differently, the smaller the mass of rock to be metasomatized for a fixed amount of fluid, the more pronounced is the effect of metasomatism on this rock.

Finally, it is geologically unreasonable that the rock system in question is closed to H_2O. Consequently, only a portion of the fluid entering rock M remains in the rock and equilibrates with it. As the result, $Y_v < 1$. Lowering of the value of Y_v lowers the effective value of X_M thus resulting in a reduction of

X_s/X_M as evaluated in Figure 6B, so that X_s/X_M is proportional to Y_v.

In applying the above considerations to the possible metasomatic alteration of REE patterns of peridotite in the portions of the upper mantle sampled by kimberlite, some information on the values of the parameters discussed above is needed. Mysen and Kushiro (1977) argued that because garnet peridotite melts under near invariant conditions, partial melting of a source rock such as GP1 will continue until one of the crystalline phases is exhausted. Consequently, depletion of GP1 to $F = 0.16$ (Table 4) is likely. The REE content of fertile garnet peridotite is likely to be in the range 1–3 relative to average chondrite (*e.g.* Shimizu, 1975a; Loubet *et al.*, 1975). From the results shown in Figure 6, it appears that $X_M > X_s$ to result in significant alteration of REE patterns of depleted garnet peridotite.

In Figure 7, calculated REE patterns of metasomatized depleted garnet peridotite are compared with the range of REE abundances found in depleted garnet peridotite. It appears from the results (Fig. 7) that $X_M > X_s$ to generate light-REE enrichment in metasomatized, depleted garnet peridotite. The range of absolute REE abundance is covered by varying the

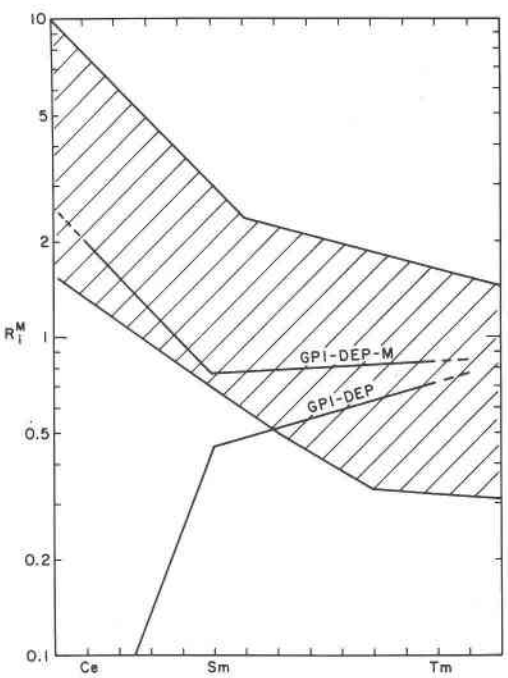

Fig. 7. REE patterns of metasomatized, depleted garnet peridotite ($F = 0.16$) at 40 kbar compared with range of values from nodules (from Fig. 5). GPI—DEP—R_i^D with $F = 0.16$ and initial R_i^s; GPI—DEP—M = GPI—DEP after metasomatism.

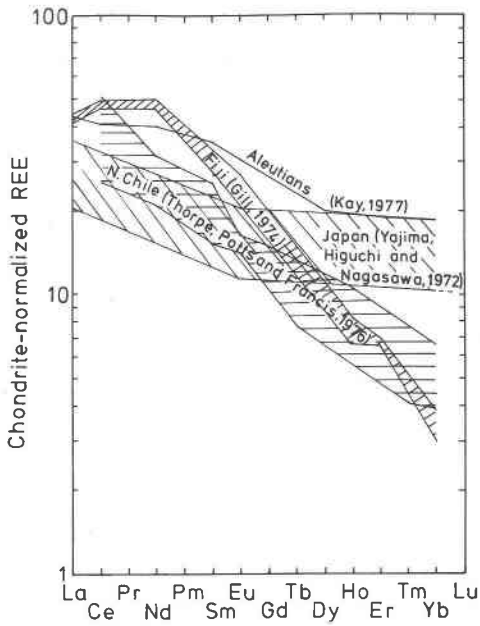

Fig. 8. Published chondrite-normalized (Schmitt *et al.*, 1963, 1964) REE patterns for island arc andesites.

R_i^s between the values commonly suggested for fertile garnet peridotite.

Island arcs

Another region of the upper mantle that may contain significant amounts of H_2O is the source region of melts beneath island arcs. High water contents of lavas in island arcs (up to 5 percent or more) have been indicated by studies of Anderson (1975) and Muenow *et al.* (1977), suggesting the presence of significant amounts of water in the source region of these melts. The trace-element geochemistry of andesitic lavas indicates enrichment in large lithophile elements (LIL) and perhaps light REE (Fig. 8), which suggests unusually large amounts of LIL elements in the source of island arc andesites or a different mineralogy compared with the source of oceanic basalts that do not show light-REE enrichment.

Most models for the formation and evolution of andesitic melts involve the presence of H_2O (see Boettcher, 1973, for a summary of these models). It has also been suggested that H_2O may play a role in governing the trace element contents of andesitic melts (Jakes and Gill, 1970; Fyfe and McBirney, 1975). Arguments have also been put forth for melting of a descending oceanic plate under essentially anhydrous conditions (*e.g.*, Marsh, 1976a,b). Marsh argued that dehydration of the plate occurred at a shallower depth than that of andesite formation. Fur-

thermore, he believed that H_2O was essentially immobile in a crystalline upper mantle. Consequently, the effect of water on the melting relations of peridotite called upon by other authors (as summarized by Boettcher, 1973) for the formation of andesite was an unlikely model. He also argued that the effect of frictional heating of the slab–mantle interface was so large that melting would occur there under any circumstance. The thermal models used in those arguments (such as calculated by Toksoz *et al.*, 1971, and Turcotte and Schubert, 1973, for example) use partial melting on the interface as a boundary condition. Petrological arguments for partial melting of a descending slab of basaltic composition based on such thermal models are therefore of questionable value because partial melting of the slab was one of the assumptions used for the thermal models.

Delaney and Helgeson (1978) cast further doubt on models for melting of the slab. They calculated the thermodynamic parameters of probable dehydration reactions that may take place in the descending plate beneath island arcs. These variables were combined with various thermal models to calculate the depth and temperature where such dehydration may occur. The pressure and temperature ranges given by Delaney and Helgeson were 25–40 kbar and 400°–600°C, respectively. It should be noted that basalt + H_2O solidi are always at temperatures greater than 600°C (*e.g.*, Robertson and Wyllie, 1971; Lambert and Wyllie, 1972; Allen *et al.*, 1975). If the results of Delaney and Helgeson are correct, dehydration of a descending plate of basaltic bulk composition may occur at depths ranging from 70 to 120 km without resulting in melting of the slab material. Provided this fluid can migrate into the overlying peridotitic wedge from the slab itself—as also argued by Jakes and Gill (1970) and Fyfe and McBirney (1975)—the trace-element content of the overlying wedge may be affected. The expected effect on REE patterns of partial melts from a metasomatized peridotitic wedge overlying dehydrating basaltic rocks in the descending plate will be considered here, and the validity of some of the preceding arguments may be assessed.

A case where amphibole, clinopyroxene, and garnet coexist with hydrous vapor in the slab is considered. Because $K_{REE}^{Amph-Cpx}$ is near 1 (Mysen, 1977a), the vapor–crystal partition coefficients of clinopyroxene and amphibole are likely to be similar. Therefore, clinopyroxene + amphibole is considered as one mineral and referred to as Cpx in the following discussion. The fluid is considered to be in equilibrium with both the dehydrating rock of eclogitic mineral assemblage and the peridotite. An uncertainty in these calculations is the temperature. According to Cullers *et al.* (1973), the vapor–crystal partition coefficients for REE increase with decreasing temperature at least at 1 kbar. If this trend also applies to REE partitioning at higher pressures, and the temperature of dehydration and metasomatism is lower than 1100°C (the experimental temperature), the bulk partition coefficients used here are minimum values. Consequently, the magnitude of the change of REE contents and patterns in peridotite beneath island arcs after passage of the metasomatic front represents minimum values.

A case where spinel peridotite (SP1; see Table 5) overlies a dehydrating slab containing amphibole, clinopyroxene, and garnet is considered. Dehydration of an amphibole-rich rock of bulk composition similar to oceanic tholeiite is likely to occur in the pressure range 20–30 kbar, resulting in a rock of eclogitic mineralogy. The fluid is considered to be in equilibrium with both the dehydrating rock of eclogitic mineral assemblage and the peridotite. The amount of released fluid (X_s), the amount of fluid in SP1 after metasomatism (X_M), and the ratio of garnet to clinopyroxene in the eclogite will affect the extent to which the REE pattern of the spinel peridotite overlying the descending plate will be affected. In the following calculations the amount of released water is varied between 0.25 and 1.0 weight percent. The amount of fluid in SP1 is also varied between 0.25 and 1 weight percent and the modal Ga/(Ga + Cpx) between 0.2 and 0.5 (Table 5). From the viewpoint of modeling bulk compositions of oceanic basalt in

Table 5. Compositional data on eclogite and garnet-free peridotite in model island arc environment

	SP1	E1	E2	E3	E4
SiO_2	47.6	53.3	52.3	51.2	50.1
Al_2O_3	2.5	5.1	7.6	10.1	12.7
MgO	47.3	20.8	21.8	23.2	24.2
CaO	2.6	20.7	18.3	15.5	13.0
		Modal Compositions			
Ga	...	20	30	40	50
Cpx	10.0	80	70	60	50
Opx	30.1	...	...	...	...
Ol	56.4	...	...	...	...
Sp*	3.5	...	...	...	...
		REE Contents**			
Ce	1	10	10	10	10
Sm	1	10	10	10	10
Tm	1	10	10	10	10

**Modal spinel evenly divided between Ol and Opx for calculation purposes.*
***Relative to average chondrite.*

CMAS, of the four compositions used, E4 is the most similar to basalt. Prior to dehydration, the slab material is considered to have an unfractionated REE pattern with REE abundances equal to ten times that of average chondrite (Schmitt *et al.*, 1963, 1964). Such REE contents are typical for oceanic tholeiite (*e.g.*, Frey *et al.*, 1974). In an open system where H_2O can move freely, the value of Y_v [equation (2)] is less than 1. Lowering of Y_v to values less than 1 would result in a shift of absolute REE abundances of the metasomatized peridotite to lower values. It is assumed, however, that as H_2O migrates into the spinel peridotite and the peridotite begins to melt, all available H_2O will dissolve in the melt. Consequently, the system is effectively closed to H_2O and $Y_v = 1$.

The REE patterns of metasomatized spinel peridotite SP1 are shown in Figure 9. The results show that an increasing proportion of garnet in the source rock results in a slight increase in the relative light-REE enrichment of SP1. A lowering of the proportion of fluid in the source rock (X_s) relative to the proportion of fluid in the metasomatized rock results in a slight increase in light-REE enrichment of SP1 (Fig. 10). Lowering of X_M results in a more rapid reduction of degree of light-REE enrichment, however (Fig. 2). The latter case would be encountered if the total mass of SP1 exceeds that of the eclogite source, whereas in the former case ($X_s < X_M$), the mass of eclogite source is less than that of metasomatized SP1.

Partial melts of similar major-element composition derived from SP1 before and after metasomatism would have different REE patterns (Fig. 11). In Figure 11, the compositions of partial melts from SP1

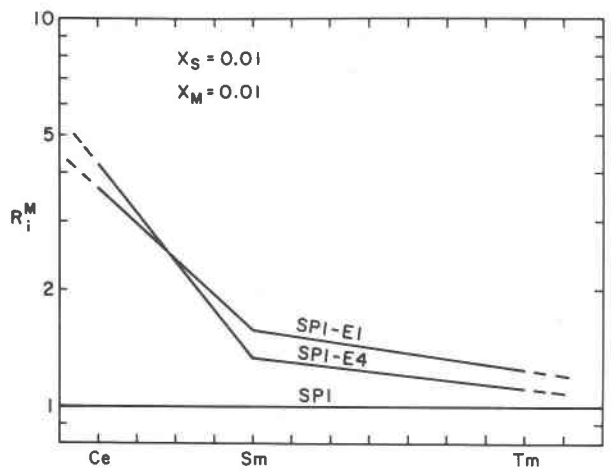

Fig. 9. REE patterns of metasomatized spinel peridotite as a function of garnet content of source rock. In this figure, $X_s = 0.01$, $X_M = 0.01$, $Y_v = 1$.

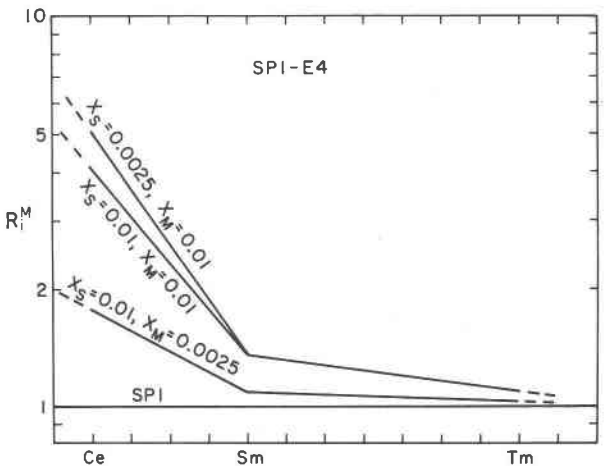

Fig. 10. REE patterns of SP1 after metasomatic alteration by fluid from source rock E4 as a function of proportion of fluid in source rock (X_s) and metasomatized rock (X_M).

and GP1 (where GP1 is garnet peridotite of similar bulk composition to SP1) with an unfractionated chondrite-normalized REE pattern equal to unity are compared with the patterns for partial melts derived from metasomatized SP1. The stoichiometry of the equation describing the melting of garnet-free peridotite is based on data of Kushiro (1969) as derived by Mysen (1977c),

$$0.54\ \text{Cpx} + 0.54\ \text{Opx} = 0.08\ \text{Ol} + \text{Liq} \qquad (4)$$

whereas equation (1) describes melting of garnet peridotite. The crystal–liquid partition coefficients for REE are from Mysen (1977a). The liquid compositions are those of an accumulated fractional melt calculated with the formulations of Shaw (1970). The use of a batch-melting model does not significantly affect the results. In this figure, 5 and 10 percent melting ($F = 0.05$ and 0.10, respectively) are considered.

Metasomatic alteration of the REE contents of spinel peridotite source rock for andesitic melts results in a light-REE enrichment of this rock that is so great that partial melts from such a rock would be more enriched in light REE and also have higher absolute REE abundances than partial melts from garnet peridotite that was not metasomatically altered prior to melting (Fig. 11). The similarity of the calculated patterns and those for natural andesite in island arcs is striking. It is concluded, therefore, that metasomatized spinel peridotite deriving its H_2O from dehydration of a descending oceanic plate with an eclogitic mineral assemblage is a likely model for andesitic formation in island arcs. The model leads to

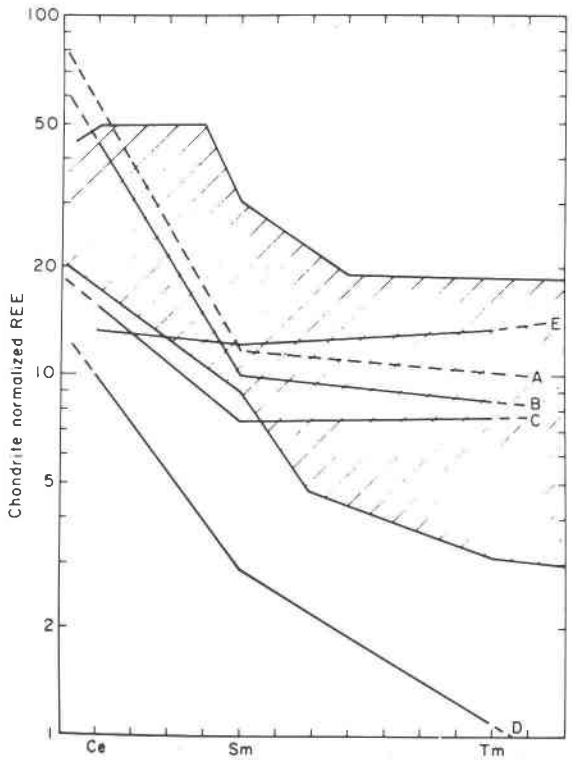

Fig. 11. REE patterns of partial melts from SP1 and GP1 compared with range of REE abundances in island arc andesite (data from Gill, 1974; Kay, 1977; Yajima *et al.*, 1972; Thorpe *et al.*, 1976). Curve A: 5 percent accumulated fractional melt from SP1-E4 with $X_s = 0.0025$, $X_M = 0.01$; Curve B: Same as A, but with 10 percent melt; Curve C: Same as B, but with $X_s = 0.01$, $X_M = 0.0025$; Curve D: 5 percent partial melt from unaltered GP1; Curve E: 5 percent partial melt from unaltered SP1.

agreement between both REE data and information on phase equilibria of wet peridotite under the appropriate pressure conditions.

Appendix

Bulk partition coefficients are defined:

$$D_i^s = \Sigma(P_i^s/K_i^{v/xt}) = \frac{(C_i^{xt})^s}{(C_i^v)^t} \quad (1)$$

$$D_i^M = \Sigma(P_i^M/K_i^{v/xt}) = \frac{(C_i^{xt})^M}{(C_i^v)^s} \quad (2)$$

where P_i^s and P_i^M *etc.* are modal proportions of phases in source rock (s) and metasomatized rock (M), respectively. The partition coefficients, $K_i^{v/xt} = C_i^{vapor}/C_i^{crystal}$, are weight ratios of element, i, in vapor and crystal.

From mass balance, for the source rock, s:

$$(C_i^{xt})^s (1 - X_s) + (C_i^v)^s X_s = R_i^s \quad (3)$$

where X_s is the proportion of s that is converted to fluid, $(C_i^{xt})^s$ and $(C_i^v)^s$ are concentrations of i in crystal and vapor in source rock, respectively. R_i^s is the total content of element, i, in rock, s.

For the metasomatized rock, M, the mass balance is:

$$R_i^M = R_i^D (1 - X_M) + (C_i^v)^s X_M \quad (4)$$

where R_i^D and R_i^M are the concentrations of element, i, before and after the fluid entered rock M. X_M is the proportion of fluid in rock M. If only a portion of the fluid (Y_v) remains in the metasomatized rock, equation (4) becomes:

$$(C_i^{xt})^M (1 - Y_v X_M) + (C_i^v)^M Y_v X_M = R_i^M \quad (5)$$

where $(C_i^{xt})^M$ and $(C_i^v)^M$ are the concentrations of i in crystals and coexisting vapor, respectively.

From equations (1) and (3):

$$(C_i^v)^s = \frac{R_i^s}{D_i^s - X_s (D_i^s - 1)} \quad (6)$$

From equations (4) and (6), the total content of element, i, in metasomatized rock, M:

$$R_i^M = R_i^D (1 - Y_v X_M) + \frac{R_i^s X_M Y_v}{D_i^s - X_s(D_i^s - 1)} \quad (7)$$

From equations (2), (5) and (7), the element contents of coexisting rock M and vapor can be calculated:

$$(C_i^{xs})^M = \frac{R_i^M}{(1 - Y_v X_M) + \frac{Y_v X_M}{D_i^M}} \quad (8)$$

Equations (7) and (8) are used in the calculations in the text.

Acknowledgments

Critical reviews by W. Harrison, J. R. Holloway, D. Rumble III, J.-G. Schilling, R. Vidale, R. J. Wendlandt, and H. S. Yoder, Jr., are appreciated.

References

Allen, J. C., A. L. Boettcher and G. Marland (1975) Amphiboles in andesites and basalt. I. Stability as a function of P–T–fO_2. *Am. Mineral., 60,* 1069–1085.

Anderson, A. T. (1975) Some basaltic and andesitic gases. *Rev. Geophys., 13,* 37–57.

Aoki, K. (1974) Chromian spinels in lherzolite inclusions from Hinome-gata, Japan. *Contrib. Mineral. Petrol., 46,* 249–256.

Boettcher, A. L. (1973) Volcanism and orogenic belts—the origin of andesite. *Tectonophysics, 17,* 231–244.

———, B. O. Mysen and P. J. Modreski (1975) Phase relationships in natural and synthetic peridotite–H_2O and peridotite–H_2O–CO_2 systems at high pressures. *Phys. Chem. Earth, 9,* 855–867.

Boyd, F. R. and J. L. England (1960) Apparatus for phase equilibrium measurements at pressures up to 50 kilobars and temper-

atures up to 1750°C. *J. Geophys. Res., 65,* 741–748.

Burnham, C. W. (1967) Hydrothermal fluids at the magmatic stage. In H. L. Barnes, Ed., *Geochemistry of Hydrothermal Ore Deposits,* p. 34–67. Holt, Rinehart, and Winston, New York.

Cullers, R. L., L. G. Medaris and L. A. Haskin (1973) Experimental studies of the distribution of rare earths as trace elements among silicate minerals and water. *Geochim. Cosmochim. Acta, 37,* 1499–1513.

Dawson, J. B. and D. G. Powell (1969) Mica in the upper mantle. *Contrib. Mineral. Petrol., 22,* 233–237.

Delaney, J. M. and H. C. Helgeson (1978) Calculation of thermodynamic consequences of dehydration in subducting oceanic crust to 100 kbar and 1000°C. *Am. J. Sci., 278,* 638–686.

Delaney, J. R., D. Muenow, J. Ganguly and D. Royce (1977) Anhydrous glass-vapor inclusions in oceanic pillow basalts (abstr.). *EOS, 58,* 530.

Eggler, D. H. (1973) Role of CO_2 in melting processes in the mantle. *Carnegie Inst. Wash. Year Book, 72,* 457–467.

——— (1974) Application of a portion of the system $CaAl_2Si_2O_8$–$NaAlSi_3O_8$–SiO_2–MgO–Fe–O_2–H_2O–CO_2 to genesis of the calc-alkaline suite. *Am. J. Sci., 274,* 297–315.

——— (1975) CO_2 as a volatile component of the mantle: the system Mg_2SiO_4–SiO_2–H_2O–CO_2. *Phys. Chem. Earth, 9,* 869–881.

——— (1976) Does CO_2 cause partial melting in the low velocity layer of the mantle? *Geology, 2,* 69–72.

——— and M. Rosenhauer (1978) Carbon dioxide in silicate melts. II. Solubilities of CO_2 and H_2O in $CaMgSi_2O_6$ (diopside) liquids and vapors at pressures to 40 kbar. *Am. J. Sci., 278,* 64–94.

Erlank, A. J. (1973) Kimberlite potassic richterite and the distribution of potassium in the upper mantle. *Extended Abstracts, International Kimberlite Conference,* University of Cape Town, p. 103–106.

——— and R. S. Rickard (1977) Potassic richterite bearing peridotites from kimberlite and evidence they provide for upper mantle metasomatism. *Extended Abstracts, Second International Kimberlite Conference,* Santa Fe, New Mexico.

——— and N. Shimizu (1977) Strontium and strontium isotope distributions in some kimberlite nodules and minerals. *Extended Abstracts, Second International Kimberlite Conference,* Santa Fe, New Mexico.

Frey, F. A., W. B. Bryan and G. Thompson (1974) Atlantic Ocean floor: geochemistry and petrology of basalts from Legs 2 and 3 of the Deep-Sea Drilling Project. *J. Geophys. Res., 79,* 5507–5527.

Fyfe, W. S. and A. R. McBirney (1975) Subduction and the structure of andesitic volcanic belts. *Am. J. Sci., 275-A,* 285–297.

Gill, J. B. (1974) Role of underthrust oceanic crust in the genesis of a Fijian calc-alkaline suite. *Contrib. Mineral. Petrol., 43,* 29–45.

Huang, W. L. and P. J. Wyllie (1976) Melting relationships in the systems CaO–CO_2 and MgO–CO_2 to 33 kilobars. *Geochim. Cosmochim. Acta, 40,* 129–132.

Irving, A. J. and P. J. Wyllie (1975) Subsolidus and melting relationships for calcite, magnesite on the join $CaCO_3$–$MgCO_3$ to 36 kb. *Geochim. Cosmochim. Acta, 39,* 35–53.

Jakes, P. and J. Gill (1970) Rare earth elements and island arc tholeiitic series. *Earth Planet. Sci. Lett., 9,* 17–28.

Kay, R. W. (1977) Geochemical constraints on the origin of Aleutian magmas. In M. Talwani and W. C. Pitmann III, Eds., *Island Arcs, Deep Sea Trenches and Back Arc Basins,* p. 229–242. American Geophysical Union, Washington, D. C.

Kennedy, G. C., G. J. Wasserburg, H. C. Heard and R. C. Newton (1962) The upper three-phase region in the system SiO_2–H_2O. *Am. J. Sci., 260,* 501–521.

Kushiro, I. (1969) The system forsterite–diopside–silica with and without water at high pressures. *Am. J. Sci., 267-A,* 269–294.

——— (1972) Effect of water on the composition of magmas formed at high pressures. *J. Petrol., 13,* 331–334.

———, N. Shimizu, Y. Nakamura and S. Akimoto (1972) Compositions of coexisting liquids and solid phases formed upon melting of natural garnet and spinel lherzolites at high pressures: a preliminary report. *Earth Planet. Sci. Lett., 14,* 19–25.

——— and H. S. Yoder, Jr. (1974) Formation of eclogite from garnet lherzolite: liquidus relations in a portion of the system $MgSiO_3$–$CaSiO_3$–Al_2O_3 at high pressure. *Carnegie Inst. Wash. Year Book, 73,* 266–269.

———, ——— and M. Nishikawa (1968) Effect of water on the melting of enstatite. *Geol. Soc. Am. Bull., 79,* 1685–1692.

Lambert, I. B. and P. J. Wyllie (1972) Melting of gabbro (quartz eclogite) with excess water to 35 kilobars, with geological applications. *J. Geol., 80,* 693–708.

Loubet, M., N. Shimizu and C. J. Allegre (1975) Rare earth elements in alpine peridotites. *Contrib. Mineral. Petrol., 53,* 1–12.

MacGregor, I. D. (1974) The system MgO–Al_2O_3–SiO_2: solubility of Al_2O_3 in enstatite for spinel and garnet peridotite compositions. *Am. Mineral., 59,* 110–119.

Marsh, B. D. (1976a) Mechanics of Benioff zone magmatism. *Am. Geophys. Union Monogr., 19,* 337–350.

——— (1976b) Some Aleutian andesites: their nature and source. *J. Geol., 84,* 27–45.

Mitchell, R. H. and D. A. Carswell (1976) Lanthanum, samarium and ytterbium abundances in some southern African garnet lherzolites. *Earth Planet. Sci. Lett., 31,* 175–178.

Muenow, D., J. R. Delaney, A. Meijer and N. Liu (1977) Water-rich glass-vapor inclusions in phenocrysts from tholeiitic pillow basalt rims in the Marianas back arc basin (abstr.). *EOS, 58,* 530.

Mysen, B. O. (1977a) Experimental determination of cerium, samarium and thulium partitioning between hydrous liquid, garnet peridotite minerals and pargasite. *Carnegie Inst. Wash. Year Book, 76,* 558–564.

——— (1977b) Magma genesis in peridotite upper mantle in light of experimental data on partitioning of trace elements between garnet peridotite minerals and partial melts. *Carnegie Inst. Wash. Year Book, 76,* 545–550.

——— (1977c) The solubility of H_2O and CO_2 in the predicted pressure and temperature range of magma genesis in the upper mantle and some petrological and geophysical implications. *Rev. Geophys., 15,* 351–361.

——— and A. L. Boettcher (1975a) Melting of a hydrous mantle. I. Phase relations of natural peridotite at high pressures and temperatures with controlled activities of water, carbon dioxide and hydrogen. *J. Petrol., 16,* 520–548.

——— and ——— (1975b) Melting of a hydrous mantle. II. Geochemistry of crystals and liquid formed by anatexis of mantle peridotite at high pressures and high temperatures as a function of controlled activities of water, hydrogen and carbon dioxide. *J. Petrol., 16,* 549–590.

——— and I. Kushiro (1977) Compositional variations of coexisting phases with degree of melting of peridotite in the upper mantle. *Am. Mineral., 62,* 843–865.

———, ——— and T. Fujii (1977) Experimental studies of diffu-

sion of water in crystalline peridotite and partitioning of some trace elements between water-rich vapor and crystals in the upper mantle. *Extended Abstracts, Second International Kimberlite Conference,* Santa Fe, New Mexico.

——— and M. G. Seitz (1975) Trace element partitioning determined by beta-track mapping—an experimental study using carbon and samarium as examples. *J. Geophys. Res., 80,* 2627–2637.

Nakamura, Y. and I. Kushiro (1974) Composition of the gas phase in Mg_2SiO_4–SiO_2–H_2O at 15 kbar. *Carnegie Inst. Wash. Year Book, 73,* 255–259.

Nixon, P. H. and F. R. Boyd (1973) Petrogenesis of the granular and sheared ultrabasic nodule suite in kimberlites. In P. H. Nixon, Ed., *Lesotho Kimberlites,* p. 48–56. Cape and Transvaal Printers, Ltd., Cape Town.

Oxburgh, E. R. (1964) Petrological evidence for the presence of amphibole in the upper mantle and its petrogenetic and geophysical implications. *Geol. Mag., 101,* 1–19.

Rhodes, J. M. and J. B. Dawson (1975) Major and trace element geochemistry of peridotite inclusions from the Lashaine volcano, Tanzania. *Phys. Chem. Earth, 9,* 545–559.

Ridley, W. I. and J. B. Dawson (1975) Lithophile trace element data bearing on the origin of peridotite xenoliths, ankaramite and carbonatite from Lashaine volcano, Tanzania. *Phys. Chem. Earth, 9,* 559–571.

Robertson, J. K. and P. J. Wyllie (1971) Rock–water systems, with special reference to the water-deficient region. *Am. J. Sci., 271,* 252–278.

Rubey, W. W. (1955) Development of the hydrosphere and atmosphere with special reference to the probable composition of the earth's atmosphere in the crust of the earth. *Geol. Soc. Am. Spec. Pap., 62,* 631–655.

Schmitt, R. A., R. H. Smith, J. E. Lasch, A. W. Mosen, D. A. Olehy and J. Vasilevski (1963) Abundances of fourteen rare-earth elements, scandium and yttrium in meteoric and terrestrial matter. *Geochim. Cosmochim. Acta, 27,* 577–622.

———, ——— and D. A. Olehy (1964) Rare-earth, yttrium and scandium abundances in meteoric and terrestrial matter, II. *Geochim. Cosmochim. Acta, 28,* 67–86.

Shaw, D. M. (1970) Trace element fractionation during anatexis. *Geochim. Cosmochim. Acta, 34,* 237–243.

Shimizu, N. (1975a) Rare earth elements in garnets and clinopyroxenes from garnet lherzolite nodules in kimberlite. *Earth Planet. Sci. Lett., 25,* 26–32.

——— (1975b) Geochemistry of ultramafic inclusions from Salt Lake Crater, Hawaii, and from southern African kimberlites. *Phys. Chem. Earth, 9,* 655–771.

Thorpe, R. S., P. J. Potts and P. W. Francis (1976) Rare earth data and petrogenesis of andesite from North Chilean Andes. *Contrib. Mineral. Petrol., 54,* 65–78.

Toksoz, M. N., J. W. Minear and B. R. Julian (1971) Temperature fields and geophysical effects of a downgoing slab. *J. Geophys. Res., 76,* 1113–1138.

Turcotte, D. L. and G. Schubert (1973) Frictional heating and the descending lithosphere. *J. Geophys. Res., 78,* 5876–5886.

Yajima, T., H. Higuchi and H. Nagasawa (1972) Variations of rare earth concentrations in pigeonitic and hypersthenic rock series from Izu-Hakone region, Japan. *Contrib. Mineral. Petrol., 35,* 235–245.

Yoder, H. S., Jr. (1950) High-low quartz inversion to 10,000 bars. *Trans. Am. Geophys. Union, 31,* 827–835.

——— (1969) Calc-alkaline andesites: experimental data bearing on the origin of their assumed characteristics. *Oregon Dept. Geol. Miner. Ind. Bull., 65,* 77–89.

Zielinski, R. A. and F. A. Frey (1974) An experimental study of the partitioning of a rare earth element (Gd) in the system diopside–vapor. *Geochim. Cosmochim. Acta, 38,* 545–565.

Manuscript received, April 24, 1978;
accepted for publication, July 25, 1978.